Title

Excess N2 and denitrification in hyporheic porewaters and groundwaters of the San Joaquin River, California.

Authors

Hinshaw, Sarra E
Zhang, Taiping
Harrison, John A
et al.

Publication Date

2020

DOI

10.1016/j.watres.2019.115161

Peer reviewed

Water Research 168 (2020) 115161

Contents lists available at ScienceDirect

Water Research

journal homepage: www.elsevier.com/locate/watres

Excess N_2 and denitrification in hyporheic porewaters and groundwaters of the San Joaquin River, California

Sarra E. Hinshaw [a, *], Taiping Zhang [b, **], John A. Harrison [c], Randy A. Dahlgren [a]

[a] University of California, Davis, Land, Air and Water Resources, One Shield Rd, Davis, CA, 95616, USA
[b] School of Environment and Energy, South China University of Technology, Guangzhou, 510006, China
[c] Washington State University Vancouver, School of the Environment, Vancouver, WA, 98686, USA

ARTICLE INFO

Article history:
Received 24 May 2019
Received in revised form
10 September 2019
Accepted 4 October 2019
Available online 5 October 2019

Keywords:
Nitrate
Membrane inlet mass spectrometer
Groundwater
Hyporheic zone

ABSTRACT

The San Joaquin River (SJR) in California is purported to receive high nitrate loadings from surrounding agricultural lands through both surface and groundwater inputs. To investigate the potential removal of nitrate (NO_3^-) from surface and ground water sources, the spatial variations in dinitrogen (N_2) gas concentrations and direct measurements of sediment denitrification potential (DNP), with amended NO_3^- and carbon (C) treatments, were investigated in the summer along a 95-km reach of the San Joaquin River. Excess N_2 in hyporheic porewaters ranged from <0.1 to 8.65 mg L^{-1} and was significantly higher in porewaters from the 1.3 m (ground water source) versus 0.3 m (mixed surface and ground water) depths. In deep groundwater wells (3–7 m), median excess N_2 concentration was 5.39 mg L^{-1} (range = <0.1 −14.6 mg L^{-1}). Excess N_2 concentrations were inversely correlated with dissolved oxygen and NO_3^- concentrations suggesting denitrification as an important process in the dominantly anaerobic sediments. Hyporheic porewater NO_3^- concentrations exceeded the detection limit of 0.01 mg L^{-1} in only 20% of the hyporheic porewaters, in spite of high NO_3^- concentrations measured in both surface waters (mean = 2.25 mg N L^{-1}) and surrounding groundwaters. Sediment DNP rates averaged 253 and 297 μg N kg^{-1} hr^{-1} for NO_3^- amended, and NO_3^- + C amended sediments, respectively, supporting the prevalence of denitrification in hyporheic sediments. Our results indicate that the hyporheic/riparian zones act as an anoxic barrier to nitrate transport from regional groundwater and as a location to remove NO_3^- from surface waters exchanging with the hyporheic zone.

1. Introduction

Anthropogenic acceleration of global nitrogen (N) fixation has led to elevated nitrate (NO_3^-) concentrations in surface and ground waters worldwide, leading to severe aquatic ecosystem degradation and drinking water impairment (Townsend et al., 2003; Galloway et al., 2004; Kulkarni et al., 2008; Schullehner et al., 2018). Riparian buffer zones and the hyporheic zone, where surface and ground waters interact with stream sediments, are recognized as important zones regulating water quality, especially the fate and transport of inorganic N forms (Muholland et al., 2008). Nutrients, oxygen and microbially-labile carbon sources interact within riparian and hyporheic zone sediments creating intermixed oxic and anoxic groundwater and porewaters, respectively, that fuel a wide range of coupled biogeochemical transformations such as denitrification, nitrification and anaerobic mineralization. The hyporheic and riparian zones predominantly act as a sink for NO_3^-, by denitrification, when NO_3^--rich surface water mixes with oxygen depleted and carbon-rich sediments and groundwater (Hill et al., 2000; Seitzinger et al., 2006).

Denitrification reduces NO_3^- to dinitrogen (N_2), with nitrite (NO_2^-), nitric oxide (NO), and nitrous oxide (N_2O) as intermediate products (Knowles, 1982). Denitrification from large rivers and lakes is an important process in the global N budget as it is estimated to account for up to 20% of total global denitrification (Seitzinger et al., 2006). Many studies have demonstrated the importance of hyporheic zone denitrification as an important sink for reactive N, attenuating N pollution's negative impacts (Seitzinger, 1988; Kulkarni et al., 2008; Merill and Tonjes, 2014). Alternative N removal pathways exist in anaerobic environments

* Corresponding author.
** Corresponding author.
E-mail addresses: shinshaw@heidelberg.edu (S.E. Hinshaw), lckzhang@scut.edu.cn (T. Zhang), john_harrison@wsu.edu (J.A. Harrison), radahlgren@ucdavis.edu (R.A. Dahlgren).

https://doi.org/10.1016/j.watres.2019.115161
0043-1354/

such as chemolithotrophic denitrification, anaerobic ammonium oxidation (anammox) and dissimilatory reduction of NO_3^- to ammonium (NH_4^+, DNRA) (Kartal et al., 2007; Marchant et al., 2016; Roland et al., 2018). DNRA does not remove N from the system but rather transforms NO_3^- to NH_4^+, whereas anammox reduces NH_4^+ and NO_2^- to N_2, resulting in the loss of N from the system (Strous et al., 1999; Burgin and Hamilton, 2007). Smith et al. (2015) found that anammox contributed 39–90% of N_2 production in groundwater and effectively removed N.

For hyporheic and riparian zone nitrate removal via denitrification, the controlling environmental factors are microbial populations, river discharge rates, residence time, organic carbon and NO_3^- supply, sediment permeability, dissolved oxygen (DO), temperature, pH, streambed sediments, and nutrient and oxygen exchange rates (O'Connor and Hondzo, 2008, Allen et al., 2007; Ishida et al., 2008; James et al., 2008). In agricultural landscapes, numerous studies show that removal of N from groundwater and surface water at the terrestrial-aquatic interface and the sediment-water interface is enhanced by the presence of abundant electron donors (namely organic carbon) and sufficient residence times to allow for microbial processing (Puckett et al., 2008; Zarnetske et al., 2011; Harvey et al., 2013).

The San Joaquin River Valley in California is one of the most intensively utilized regions in the world for irrigated agriculture, receiving high N inputs from fertilizers, agricultural drainage, livestock operations, atmospheric deposition, urban wastewater and stormwater discharge resulting in a history of surface and groundwater contamination (Burow et al., 1998; Kratzer et al., 2004; Tomich et al., 2016). Surface water NO_3^- concentrations in the lower portion of the SJR generally range between 1 and 4 mg N L^{-1} and contribute to eutrophication and seasonally hypoxic conditions in portions of the lower river (Kratzer et al., 2004). Groundwater NO_3^- concentrations are elevated throughout much of the SJR Valley, often exceeding the drinking water standard of 10 mg N L^{-1} (Harter et al., 2017). Given the high NO_3^- concentrations found in the surrounding groundwaters of the lower SRJ Valley, it was inferred that NO_3^- loads from groundwater sources could contribute appreciably to surface water NO_3^-. Thus, distinguishing groundwater N contributions to surface waters and understanding the relative importance of groundwater-surface water interactions in controlling NO_3^- transport are important for developing basin-wide, agricultural water quality management plans to reduce nutrient loads in the lower SJR.

Nitrogen dynamics in streams and rivers are not well-understood, in-part because it is difficult to measure dynamic N removal processes across time and space (Groffman et al., 2006). The intent of this study is not to distinguish between N removal pathways but rather to use excess N_2 (an end-product of several major N removal pathways) as an indicator of reactive N removal at the landscape scale. We use a combination of membrane inlet mass spectrometer (MIMS) derived N_2 supersaturation estimates and potential denitrification assays (acetylene inhibition technique) from hyporheic sediments to assess removal of nitrate, as well as the factors limiting this removal. Measurements of N_2 using MIMS technology allow for quantification of net N_2 accumulation independent of the metabolic pathway and represent an integration of all N biogeochemical processes taking place along the groundwater flowpath (Kana et al., 1994; Blicher-Mathiesen et al., 1998; Weymann et al., 2008). The use of the acetylene inhibition technique allows for measurements of potential rates and manipulations of sediments to assess controlling factors. In this study we: i) investigated spatial variability in excess N_2 within hyporheic zone porewaters and groundwater wells along a 95-km reach of the lower SJR, ii) assessed the relationship between nitrate concentrations and other physio-chemical characteristics on excess N_2 concentrations, and iii) examined the denitrification potential of hyporheic sediments via acetylene inhibition along the lower SJR. In so doing, we provide some of the first estimates of the importance of N removal in surface and groundwaters of the SJR, and provide an example of how such an approach can be used to understand landscape scale N removal distribution and dynamics.

2. Material and methods

2.1. Overview

In order to enhance understanding of the spatial distribution of N removal in the SJR, we measured N_2:Ar ratios in 168 hyporheic zone porewater samples (0.31–1.82 m depth) from 28 sites over a 95-km reach during summer low flow conditions. Sampling in other seasons was not possible due to high flow. These samples were augmented with groundwater samples from three locations with nested wells ranging in depth from 3 to 7 m. Results from the N_2:Ar experiment warranted further investigation into sources of N_2 therefore an acetylene inhibition experiment was conducted the following year to establish what factors were likely limiting denitrification and to estimate potential denitrification rates using hyporheic sediments from six sites. Table S1 provides a summary of sampling and analytical approaches.

2.2. Study sites

This study was conducted along a 95-km section of the lower San Joaquin River California between the confluence of Salt Slough (river km = 211) and Vernalis (116 km) (37″18′31″ N, 120″55′44″ W and 37″40′34″N, 121″15′55″W) (Fig. 1). Within the study reach, the SJR has a low gradient (0.0156%) and a generally coarse to medium sandy substratum with infrequent clay and silt deposits. Mean monthly river discharge varies seasonally from 41 to 214 $m^3 s^{-1}$ (USGS, 2011). The Merced, Tuolumne and Stanislaus tributaries contribute 79% of SJR flow with the remainder from subsurface drainage and irrigated agriculture return flows (Kratzer et al., 2004). Land-use in the lower SJR Valley is dominated by agriculture with orchard, vineyards, cropland and pasture. Within the study area, climate is arid-to-semiarid receiving 254–305 mm of annual precipitation, mainly in winter. Long-term trends in water quality and a complete description of the study area can be found in Kratzer et al. (2004) and Zamora et al. (2012).

2.3. Field methods

A total of 28 sites were chosen along the river reach to target specific river conditions (Zamora et al., 2012) and 168 hyporheic porewater samples (28 sites x 3 cross-section sites x 2 depths) were collected between August 11 and 21, 2008 (Fig. 1). At each site, hyporheic porewater was collected at 0.31 and 1.82 m depths for three positions across the river cross-section: 20% (east), 50% (middle) and 80% (west) channel widths. Sampling of the west (80%) and east (20%) sides of the river channel was designed to examine potential differences resulting from contrasting soil/aquifer materials. West-side deposits are generally fine textured (loams) originating from sedimentary deposits in the Coastal Ranges, while east-side deposits are coarse textured (sandy) originating primarily from granitic rocks in the Sierra Nevada (Galloway and Riley, 1999). Porewater was extracted with a peristaltic pump connected to a temporary drive point (piezometer: 0.95-cm diameter stainless-steel tube with 0.04-cm slots). Dissolved oxygen, pH, temperature and specific conductivity (SC) were measured using a 556 YSI sonde (YSI, Yellow Springs, OH) mounted in a flow through cell which received continuously pumped water from the

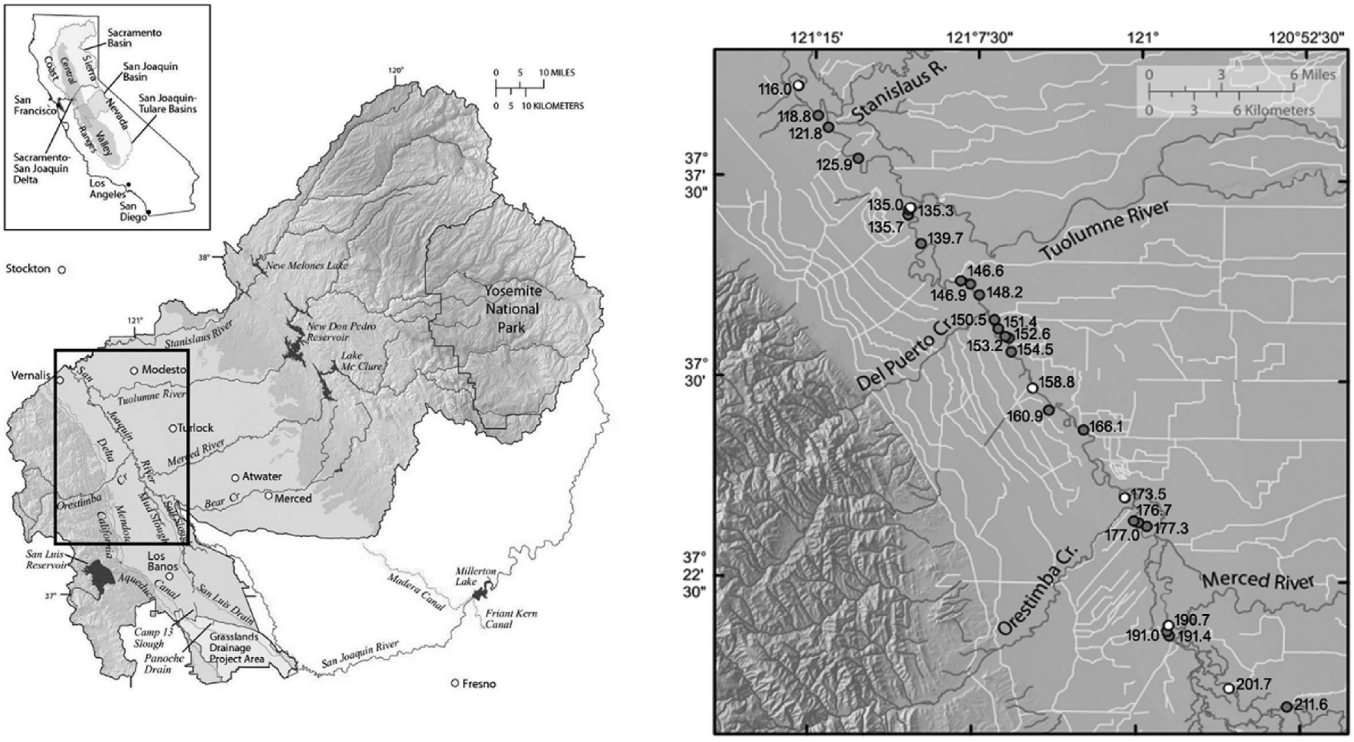

Fig. 1. The San Joaquin Basin and location of sampling sites in the San Joaquin River. Open circles represent denitrification potential experiment sites (Zamora et al., 2012).

piezometer. Following attainment of stable water quality parameters, a water sample for dissolved gas analysis (N_2:Ar) was collected by a peristaltic pump from the piezometers into a 120 mL glass bottle following USGS gas sampling protocols (https://water.usgs.gov/lab/dissolved-gas/sampling/). Samples were preserved with 15 mg of potassium hydroxide, sealed with a butyl rubber septum and a crimp top seal, and inspected to assure that no bubbles were present. Sample bottles were stored upside down to keep any bubbles that formed away from the stopper and submerged in water at 4 °C until analysis. Additionally, a 60 mL sample was filtered through a 0.2 μm polycarbonate membrane filter for nutrient analysis from each porewater depth and from surface waters.

In addition to the longitudinal hyporheic sampling, water samples were collected from groundwater wells (5-cm diameter PVC construction) at three sites (190.7, 173.5 and 158.8 km) on the east and west banks of the SJR at depths of 3–7 m (Zamora et al., 2012). Groundwater was collected using a submersible-inline pump (LVM Congo/Amazon, Arlesey, Bedfordshire, UK) after purging three well casings of water. Groundwater samples for dissolved N_2:Ar and general water chemistry were collected in the same manner as described above for porewaters.

2.4. Dissolved N_2:Ar gas analysis

Dissolved gas samples collected from hyporheic porewaters and groundwater were analyzed with a membrane-inlet mass spectrometer (MIMS) (Kana et al., 1994) and analyzed using solubility constants of Weiss and Price (1980). Prior to analysis, porewater samples were brought to room temperature in a water bath to equilibrate the dissolved gases and eliminate any air bubbles formed during refrigeration and storage. Five pseudo-replicated readings were taken from each sample for N_2:Ar quantification and replicates had a coefficient of variation $\leq$0.003%. Deionized water equilibrated with the atmosphere was used as a standard and temperature was set within 2 °C of field-measured water temperatures (Kana et al., 1994). The N_2:Ar method measures the total net N_2 flux produced by denitrification or consumed by N_2 fixation. Positive values above the expected atmospheric equilibrium of porewater samples contained excess N_2 (Heaton and Vogen, 1981; Holocher et al., 2002). N_2:Ar ratios were converted to excess N_2 mg L^{-1} based on Kana et al. (1994) and Harrison et al. (2005).

2.5. Sediment denitrification potential

Sediments were collected from six sites (201.7, 190.7, 173.5, 158.8, 135.0 and 116.0 km) along the lower SJR in April and September 2009 (Fig. 1). At each site, duplicate sediment samples, each consisting of four composite cores (18 × 9.5 cm v = 200 mL), were collected from three river cross section sites (20, 50 and 80% widths) and two depths (5–15 and 15–30 cm). The samples were homogenized and placed in a heavy-duty polyethylene freezer bag, airspace purged and sealed, placed in a second zip-lock bag and place on ice for transport. Surface water was collected from all sites and filtered through a 0.2 μm polycarbonate membrane filter for nutrient analysis.

DNP was determined using the acetylene block technique (Tiedje, 1982) within 48 h of sample collection. Duplicate sediment samples from each depth and site were measured to 25 g subsamples of sediment slurry and placed in 125 mL Erlenmeyer flasks to establish NO_3^-- addition and NO_3^-- + C addition treatments. Site water was added based on moisture content for a 1:1 ratio of dry soil to water weight. DNP was negligible in ambient samples due to the lack of NO_3^- in the sediments and therefore ambient DNP results are not reported. The NO_3^- and NO_3^-- + C addition treatments were established by adding 200 NO_3^- mg N L^{-1} and 200 mg C L^{-1} of

glucose combined with 200 NO_3^- mg N L^{-1}, respectively. All assays contained chloramphenicol (1 g L^{-1}) to inhibit microbial growth during the incubation period.

Flasks were capped with stoppers, evacuated and flushed with high-purity N_2 gas at a flow rate of 1.5 L min^{-1} for two minutes. A 15-mL volume of gas inside the flasks was removed and 15 mL of acetylene was injected in its place. Slurries were incubated at room temperature (24 ±1 °C) on a shaker table. Headspace gas samples (1 mL) were collected at 30, 60 and 90 min after acetylene injection. Gas samples were placed in 6-mL evacuated Exetainer vials, and analyzed for N_2O on a Hewlett Packard 3600 gas chromatograph with an electron capture detector (ECD). DNP rates were determined by linear regression of the three time points ($r^2 > 0.95$) and corrected with the Bunsen absorption coefficient to estimate total N_2O (Weiss and Price, 1980; Tiedje, 1982).

2.6. Sediment and water chemistry characterization

Surface water, hyporheic porewater, and groundwater samples were analyzed for NO_3^-, NO_2^-, NH_4^+, phosphate (PO_4^{3-}), and dissolved organic carbon (DOC) following filtration through a 0.2 μm polycarbonate membrane filter (Millipore). Hydrochloric acid was added to DOC samples immediately after filtration (pH < 2). The vanadium chloride method was used to spectroscopically determine NO_3^- + NO_2–N and NO_2–N (Limit of detection (LOD) = 0.01 mg L^{-1}) (Doane and Howarth, 2003). NH_4–N was determined spectroscopically with the Berthelot reaction, using a salicylate analog of indophenol blue (LOD ~ 0.01 mg L^{-1}; Forster, 1995). Dissolved-reactive PO_4–P was determined using the ammonium molybdate spectrophotometric method (LOD ~0.005 mg LP^{-1}; Eaton et al., 1998). DOC was measured using a Dohrmann UV enhanced-persulfate TOC analyzer (Phoenix 8000; Teledyne Tekmar; LOD ~0.1 mg L^{-1}).

Sediment moisture content was determined by oven drying at 60 °C for 72 h. TOC and oxidizable organic carbon (OxC) were measured on air-dried, homogenized sediment samples. TOC and total N (TN) were analyzed using a Costech ECS 4010 CHNSO Analyzer (Costech Analytical Technologies, California, USA). OxC was measured by the modified permanganate method (Weil et al., 2003). Particle-size distribution (PSD) was determined using a Beckman-Coulter LS-230.

2.7. Statistical analysis

Homogeneity of variance was tested with Levene's test and, if necessary, data were log or log +1 transformed. General linear model ANOVAs were performed to test differences in excess N_2 concentrations and water chemistry, with sites, depths and cross-sectional position as main factors ($p < 0.05$). Least significant difference (LSD) post-hoc tests were used to separate means if significant differences existed between positions or sites. Linear regression was used to examine correlations among independent physical and chemical variables and excess N_2 concentrations or DNP rates. Percent NO_3 loss to N_2 was calculated as excess N_2/(NO_3 + N_2)*100 and the proportion of N_2 from DIN d = ++was calculated as excess N_2/(NO_3 + NH_4 + NO_2+N_2)*100. One-way ANOVA's were performed to investigate differences in DNP rates and sediment/surface water characteristics. A paired *t*-test established differences in porewater chemistry and DNP rates between depths (shallow and deep) and groundwater positions (east and west). All statistical analyses were preformed using SPSS 20 (SPSS, 2001). Data are reported as mean ± standard error (SE) unless otherwise stated.

3. Results

3.1. Hyporheic porewater and surface water characteristics

River discharge in August 2008 ranged from 1.67 $m^3 s^{-1}$ at 211.6 km to 24.6 $m^3 s^{-1}$ for the most downstream site at 116.0 km. Water depth at the time of sampling ranged from 0.15 to 1.4 m. Porewater temperatures ranged from 17.8 to 30 °C (23.7 ± 0.16 °C), generally decreasing in the downstream direction with significantly higher temperatures at shallow depths ($p < 0.001$) (Table 1). Specific conductivity ranged from 0.62 to 16.3 mS cm^{-1} (2.70 ± 0.16 mS cm^{-1}). Porewater DOC concentrations ranged from <0.1 to 14.4 mg C L^{-1} (median = 1.9 mg C L^{-1}) with decreasing concentrations downstream and significantly higher concentrations in shallow, west channel porewaters. Only 20% of NO_3^- concentrations exceeded the detection limit (0.01 mg N L^{-1}), with a few sites (177, 176.7 and 154.5 km) having >10 mg N L^{-1} in the middle and east channel positions. NH_4^+ concentrations ranged between <0.01 and 22 mg N L^{-1} (median = 0.34 mg N L^{-1}). Dissolved O_2 concentrations ranged from 0.36 to 5.8 mg L^{-1} (4.1–38% saturation, mean = 11.1 ± 0.16% saturation) with a median of 0.86 mg L^{-1} demonstrating that most sites were hypoxic (<2 mg L). Hyporheic sediments at depths greater than 5 cm consistently displayed visual evidence of iron and/or sulfur reduction (e.g., gleyed or black sulfidic coloration & odorous) confirming the predominance of anoxic conditions (Fig. S1). DO concentrations in porewaters were significantly different ($p = 0.04$) between shallow (0.31 mean = 1.12 ± 0.09 mg L^{-1}) and deep (1.82 mean = 0.98 ± 0.09 mg L^{-1}) depths.

Surface water DOC concentrations ranged from 2.8 to 7.0 mg L^{-1} (mean = 4.0 ± 0.14 mg L^{-1}), NO_3^- ranged from 0.71 to 3.62 mg N L^{-1} (2.28 ± 0.17 mg L^{-1}), and SC in surface waters was lower than porewater concentrations ranging from 0.58 to 1.57 mS cm^{-1} (0.97 ± 0.17 mS cm^{-1}) (Fig. 2, Table S2). NH_4^+-N ranged from <0.01 to 0.07 mg L^{-1} (0.02 ± 0.02 mg L^{-1}). All surface water samples were well oxygenated, but O_2 concentrations were highly dependent on time of day (DO saturation: median = 117% (range 59–157%).

3.2. Excess dissolved N_2 in hyporheic porewaters

Of the 168 porewater samples measured, 71% contained dissolved N_2 above temperature-adjusted, atmospheric equilibrated values; the remaining samples were at or slightly negative with respect to equilibrium (due to variations in O_2, see Lunstrum and Aoki, 2016). Excess N_2 concentrations ranged from <0.1 to 8.65 mg N L^{-1} with the highest concentrations (mean = 5.81 ± 0.92 mg N L^{-1}) observed at 139.7 km (Fig. 3). One-way ANOVA tests found excess N_2 was significantly different among sites ($p < 0.001$) and between depths ($p < 0.012$). At most sites, excess N_2 at 1.82 m depth was greater than at 0.31 m depth. In the upstream sites, excess N_2 was low in shallow porewaters with a general pattern of increasing excess N_2 with distance downstream. Excess N_2 concentrations were significantly different ($p = 0.048$) between cross-section positions with shallow depths following west (1.71 ± 0.28) > middle (1.55 ± 0.23) > east (1.35 ± 0.19) and deep depths following west (2.92 ± 0.45) > middle (2.36 ± 0.40) > east (2.14 ± 0.36). Excess N_2 was negatively correlated with temperature (r^2 = -0.17, $p < 0.001$) and showed a weak inverse relationship to DO and NO_3^- concentrations (r^2 = -0.12, $p = 0.002$; r^2 = -0.10, $p = 0.003$). Linear regression showed a strong negative correlation between excess N_2 and NO_3^- concentrations when NO_3^- was >0.1 mg N L^{-1} with both depths (r^2 = -0.41, $p < 0.001$) and was best fit within shallow porewater samples when NO_3^- concentrations were >0.1 mg N L^{-1} (r^2 = -0.80, $p < 0.001$, Fig. 4).

Table 1
Porewater characteristics from San Joaquin River study sites. Values represent the range, mean and standard error of six replicates.

Site	Temperature (°C)		N_2 (mg L^{-1})		NO_3^--N mg L^{-1}		NH_4^+-N mg L^{-1}		DOC mg L^{-1}		DO mg L^{-1}		SC mS cm^{-1}	
211.6	22.6–26.8	24.6 (0.8)	0.00–1.09	0.18 (0.2)	<0.01	0.00 (0.0)	0.03–1.47	0.65 (0.2)	3.81–8.18	4.90 (0.7)	0.80–2.70	1.28 (0.3)	3.83–4.63	4.03 (0.1)
201.7	23.2–27.5	25.5 (0.7)	0.00–0.67	0.25 (0.2)	<0.01	0.00 (0.0)	0.74–2.38	1.30 (0.3)	3.02–9.63	4.93 (1.0)	0.61–1.70	1.15 (0.2)	4.00–16.3	6.62 (1.9)
191.4	25.1–26.2	25.8 (0.2)	0.00–1.78	0.36 (0.3)	<0.01	0.00 (0.0)	0.03–2.25	0.57 (0.4)	0.72–8.12	5.35 (1.1)	0.95–1.13	1.03 (0.0)	0.70–5.86	1.80 (0.8)
191	24.3–27.8	26.1 (0.6)	0.40–0.90	0.62 (0.1)	<0.01–2.28	0.67 (0.4)	<0.01–0.95	0.42 (0.2)	0.36–2.99	1.28 (0.4)	0.85–1.40	1.14 (0.1)	1.31–4.81	2.93 (0.5)
190.7	24.4–28.6	26.0 (0.8)	0.00–2.65	1.04 (0.5)	<0.01–0.02	0.00 (0.0)	0.02–11.6	4.20 (2.2)	0.63–13.6	5.76 (2.4)	0.84–1.17	1.03 (0.1)	2.20–5.00	3.28 (0.4)
177.3	22.0–26.0	24.0 (0.7)	0.00–2.22	0.83 (0.4)	<0.01–0.00	0.00 (0.0)	0.24–3.26	1.08 (0.5)	2.09–4.66	2.96 (0.4)	0.70–0.96	0.86 (0.0)	1.78–2.14	1.96 (0.0)
177	22.0–25.2	23.6 (0.5)	0.00–4.10	1.74 (0.7)	<0.01–13.9	5.04 (2.7)	<0.01–0.59	0.15 (0.1)	1.00–1.74	1.38 (0.1)	0.48–1.81	1.00 (0.2)	1.44–2.04	1.77 (0.1)
176.7	21.9–26.7	23.8 (0.7)	0.00–2.92	0.98 (0.5)	<0.01–14.3	6.01 (2.2)	<0.01–19.6	3.28 (3.3)	0.90–14.4	3.45 (2.2)	0.69–3.31	1.78 (0.4)	1.50–2.24	1.90 (0.1)
173.5	22.1–25.1	23.5 (0.4)	0.00–2.93	1.34 (0.5)	<0.01–4.47	1.96 (0.8)	<0.01–0.13	0.04 (0.0)	0.33–1.31	0.86 (0.2)	0.50–5.67	2.27 (1.0)	0.62–3.74	1.83 (0.6)
166.1	22.4–25.4	23.7 (0.4)	0.00–1.23	0.26 (0.2)	<0.01	0.00 (0.0)	0.10–1.44	0.39 (0.2)	1.06–2.17	1.49 (0.2)	0.50–0.80	0.60 (0.1)	3.89–4.79	4.45 (0.2)
160.9	20.9–25.6	23.5 (0.8)	0.00–3.38	1.71 (0.6)	<0.01	0.00 (0.0)	0.01–0.09	0.04 (0.0)	1.25–1.92	1.50 (0.1)	0.59–1.00	0.85 (0.2)	2.78–3.65	3.10 (0.2)
158.8	23.5–26.7	25.3 (0.5)	1.03–3.36	2.23 (0.4)	<0.01–0.29	0.05 (0.1)	0.06–14.4	3.59 (2.3)	1.93–5.19	3.31 (0.5)	0.65–1.40	1.05 (0.1)	0.97–3.41	2.11 (0.4)
154.5	23.0–25.7	24.5 (0.4)	0.00–0.73	0.23 (0.1)	6.32–12.7	10.3 (1.2)	<0.01–0.01	0.00 (0.0)	0.80–2.06	1.36 (0.2)	0.79–2.93	1.29 (0.3)	2.00–3.13	2.46 (0.2)
153.2	20.7–24.3	22.4 (0.7)	0.00–3.85	0.72 (0.8)	<0.01	0.00 (0.0)	0.37–6.45	3.26 (1.1)	1.53–6.12	4.20 (0.8)	0.69–1.84	1.00 (0.2)	1.29–1.85	1.42 (0.1)
152.6	21.4–25.6	22.9 (0.6)	0.00–3.86	1.33 (0.7)	<0.01	0.00 (0.0)	0.16–3.65	1.57 (0.7)	2.64–7.31	4.77 (0.8)	0.69–1.03	0.84 (0.1)	1.08–1.60	1.31 (0.0)
151.4	19.0–23.1	21.0 (0.7)	0.85–3.53	2.05 (0.5)	<0.01–0.01	0.00 (0.0)	0.25–0.64	0.52 (0.1)	1.98–2.53	2.32 (0.1)	0.92–2.17	1.36 (0.2)	1.36–1.61	1.46 (0.0)
150.5	21.6–25.0	23.3 (0.6)	0.00–4.81	1.92 (0.7)	<0.01–0.06	0.02 (0.0)	0.02–0.86	0.25 (0.1)	0.78–3.04	1.73 (0.3)	0.56–1.05	0.80 (0.1)	1.58–2.16	1.90 (0.1)
148.2	21.6–25.2	23.8 (0.7)	0.00–3.54	1.46 (0.5)	<0.01–0.00	0.00 (0.0)	0.03–14.9	2.76 (2.4)	0.54–9.42	3.18 (1.3)	0.59–1.13	0.86 (0.1)	1.28–2.21	1.70 (0.2)
146.9	19.5–24.3	22.2 (0.7)	0.00–3.98	2.27 (0.6)	<0.01–1.31	0.22 (0.2)	0.01–0.54	0.28 (0.1)	0.63–2.67	1.58 (0.3)	0.56–0.89	0.75 (0.1)	0.67–1.54	1.13 (0.2)
146.6	22.6–26.8	22.0 (0.6)	0.00–2.43	1.09 (0.6)	<0.01	0.92 (0.9)	0.03–1.47	0.13 (0.0)	3.81–8.18	0.93 (0.3)	0.80–2.70	0.60 (0.1)	1.29–2.74	1.78 (0.3)
139.7	21.9–24.7	23.5 (0.5)	3.22–8.65	5.81 (0.9)	<0.01	0.00 (0.0)	0.06–3.90	0.86 (0.6)	2.63–4.58	3.24 (0.3)	0.49–1.44	0.78 (0.1)	2.27–3.46	2.90 (0.2)
135.7	20.4–23.5	22.0 (0.5)	1.51–4.52	2.79 (0.4)	<0.01	0.00 (0.0)	0.34–0.74	0.56 (0.1)	0.01–0.54	0.21 (0.1)	0.57–0.87	0.71 (0.0)	5.94–10.2	8.19 (0.8)
135.3	22.9–25.3	24.0 (0.5)	0.36–3.10	1.76 (0.4)	<0.01	0.00 (0.0)	0.93–3.23	1.76 (0.2)	0.00–3.67	1.38 (0.5)	0.56–0.73	0.64 (0.0)	1.35–8.03	4.40 (1.3)
135	24.0–25.8	25.2 (0.3)	0.00–3.27	1.44 (0.5)	<0.01–0.04	0.01 (0.0)	1.39–22.0	8.02 (3.2)	0.47–8.35	3.64 (1.1)	0.57–1.2	0.85 (0.1)	1.23–6.15	3.00 (0.8)
125.9	17.8–25.1	22.1 (1.1)	0.00–6.50	1.59 (1.0)	<0.01–0.18	0.03 (0.0)	0.04–0.95	0.56 (0.2)	0.97–2.98	1.93 (0.3)	0.85–5.00	1.85 (0.7)	1.68–1.96	1.81 (0.0)
121.8	20.3–24.0	22.2 (0.5)	0.03–4.48	2.56 (0.7)	<0.01	0.00 (0.0)	0.01–1.05	0.40 (0.2)	0.86–2.66	1.68 (0.3)	0.58–1.17	0.81 (0.1)	1.11–2.80	2.19 (0.3)
118.8	22.1–24.2	23.2 (0.3)	1.13–4.10	2.26 (0.4)	<0.01–3.85	0.93 (0.6)	0.02–0.24	0.14 (0.0)	0.76–1.10	0.91 (0.1)	0.55–0.84	0.69 (0.0)	2.29–2.38	2.39 (0.0)
116	22.1–24.7	23.4 (0.4)	0.00–3.20	1.53 (0.5)	<0.01	0.00 (0.0)	0.05–4.95	1.37 (0.8)	1.29–2.81	2.03 (0.2)	0.36–4.33	1.67 (0.8)	0.74–3.31	1.85 (0.5)

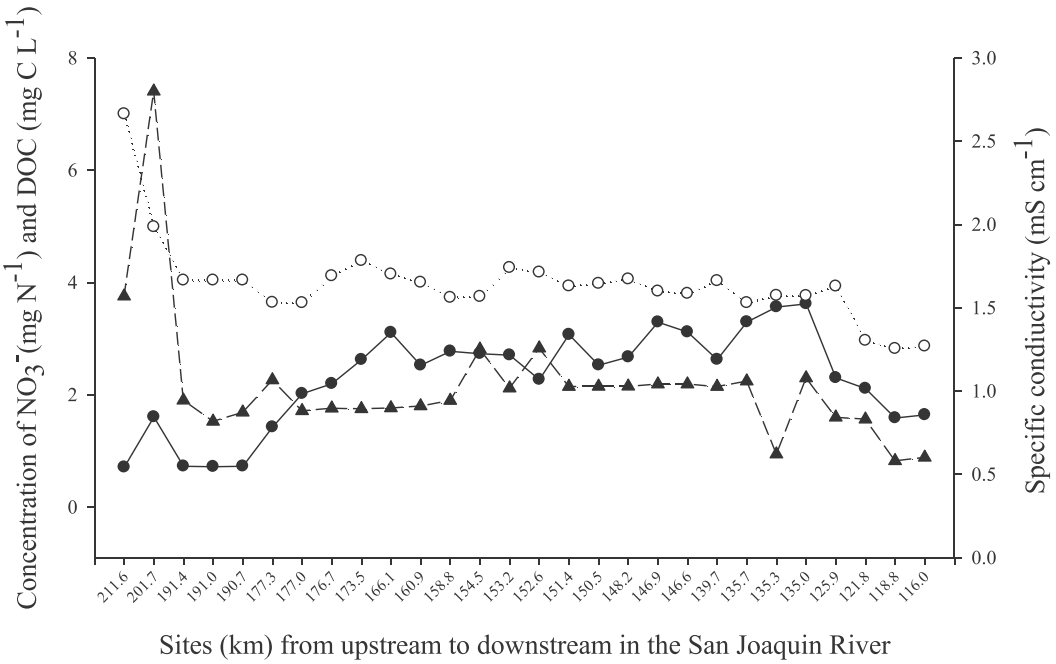

Fig. 2. Concentrations of NO_3^-, DOC and SC in surface waters along the 95 km of the lower San Joaquin River.

3.3. Surface water and sediment characteristics for DNP analysis

River discharge in April 2009 ranged from 5.49 $m^3 s^{-1}$ at 201.7 km to 39.2 $m^3 s^{-1}$ and was significantly lower in September 2009 ranging from 2.61 $m^3 s^{-1}$ to 31.3 $m^3 s^{-1}$ ($p = 0.02$). Within surface waters, SC ranged between 0.39 and 1.05 mS cm^{-1} with generally decreasing values from upstream to downstream (Table 2). Surface water NO_3^- concentrations were highest at Site 135 in April and 158.8 in September with a maximum concentration of 3.03 mg N L^{-1}. Total organic carbon concentrations in sediment ranged from 0.04 to 1.25% (mean = 0.27 ± 0.04) whereas TN was considerably lower with an average of 0.03% ± 0.01. Oxidizable carbon concentrations were significantly different between sampling seasons; higher concentrations occurred in September (223 ± 43 mg kg^{-1}) than in April (159 ± 43 mg kg^{-1}, Table 3). Both TOC and OxC concentrations were significantly different among

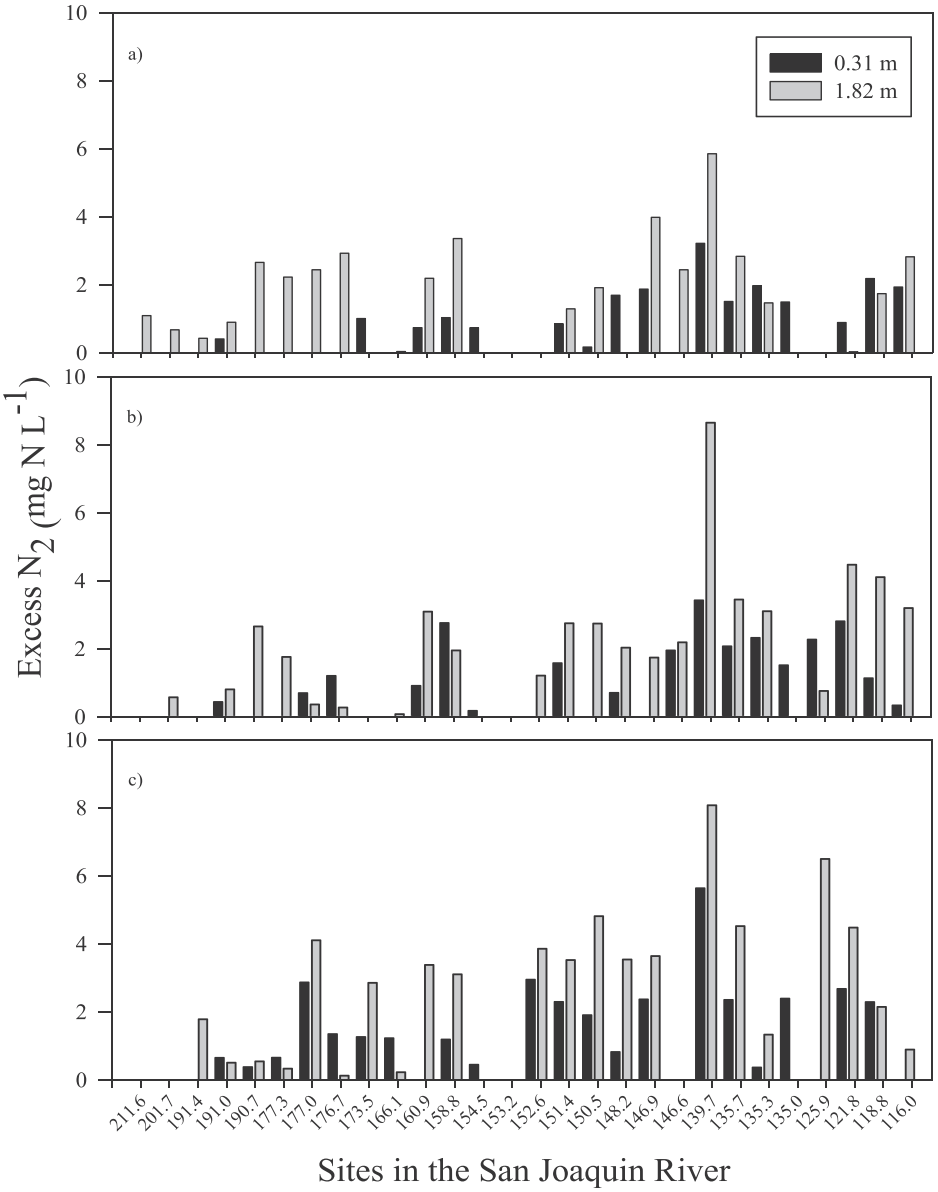

Fig. 3. N_2 concentrations in porewater collected from a) 20% (east), b) 50% (middle) and c) 80% (west) of the river width along a 95 km stretch of the San Joaquin River.

sites with the highest concentrations at Site 173.5 km ($p < 0.001$, mean = 0.43% ± 14 and 301 ± 101 for TOC and OxC). Particle-size distribution ranged between coarse silt and coarse sand (58.3–777.8 μm) with Site 173.5 and 158.8 km having a significantly smaller particle size ($p < 0.001$, Table 3).

3.4. Denitrification potential (DNP) rates

DNP rates were <0.01–4308 (261.9 ± 134 μg N kg^{-1} hr^{-1}) and <0.01–6101 (323.2 ± 181 μg N kg^{-1} hr^{-1}) for the NO_3^- amended and NO_3^- + C amendments, respectively, with no significant differences between treatments (Fig. 5) or seasons. Amended DNP rates for both NO_3^- and NO_3^- + C were significantly different among sites and within river cross section positions, with significant interactions found between these two main factors ($p < 0.001$). The highest DNP rates (>1000 μg N kg^{-1} hr^{-1}) occurred at Site 173.5 km in the west channel. The other five sites were not significantly different from one another but they were all significantly different than site 173.5 km. DNP rates were lowest in the east channel (56.4 ± 18.6 and 66.7 ± 20.0 μg N kg^{-1} hr^{-1} for NO_3^- and NO_3^- + C treatments, respectively) with significantly higher rates in the west channel (619.6 ± 386 and 794 ± 526 μg N kg^{-1} hr^{-1} for NO_3^- and NO_3^- + C treatments, respectively). No significant differences were found between the 5–15 and 15–30 cm depths.

The combined data for DNP rates in NO_3^- and NO_3^- + C amended treatments were significantly related to %TOC ($r^2 = 0.52$, $p < 0.001$), %TN ($r^2 = 0.56$, $p < 0.001$) and OxC concentrations ($r^2 = 0.57$, $p < 0.001$) (Fig. 6). Stepwise regression suggested that OxC was the main limiting factor regulating DNP rates. When the exceptionally high rates from site 173.5 km were removed from the analysis, an inverse relationship was found with PSD ($r^2 = 0.63$, $p < 0.001$).

3.5. Permanent groundwater wells

The pH within permanent groundwater wells ranged from 6.6 to 7.5. Specific conductivity and temperature ranged from

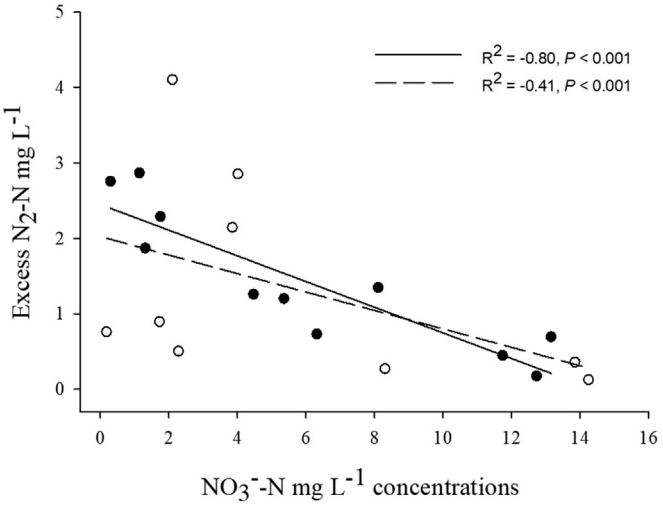

Fig. 4. Open circles indicate 1.82 m depth and closed circles represent 0.31 m depth. The dashed regression line represents the relationship when NO_3^- concentrations for all porewater samples are included and >0.1 mg N L^{-1} and the solid regression line represent the relationship when NO_3^- concentrations were >0.1 mg N L^{-1} at 0.31 m.

0.13 → 2.71 mS cm^{-1} and from 19.0 → 20.4 °C, respectively. DO ranged from 0.03 to 0.22 mg L^{-1} (mean = 0.14 ± 0.04) and DOC concentration was generally low (0.68 → 2.34 mg C L^{-1}; (Table S3). Concentrations of DO and DOC were negatively correlated ($r^2 = 0.75$, $p = 0.02$). Excess N_2 ranged from <0.1 to 14.6 mg N L^{-1} (Table S3) with no significant differences found among sites or east versus west bank positions. Although there were no significant differences, mean excess N_2 in west bank wells (9.8 ± 2.5 mg N L^{-1}) was 3 times greater than concentrations in east bank wells. A strong negative relationship was found between excess N_2 and NO_3^- concentrations ($r^2 = -0.85$, $p = 0.03$). No significant relationships were found between excess N_2 and any of the other measured water chemistry parameters.

4. Discussion

4.1. Excess N_2 in hyporheic porewater and groundwater wells

This study was conducted on the lower portion of SJR over a distance of 95 km. The use of dissolved N_2:Ar ratios allowed us to assess the cumulative amount of excess N_2 occurring within porewater and adjacent groundwater wells. Excess N_2 concentrations in the SJR were greater than those reported from other agriculturally impacted rivers (range = 0.01–0.47 mg N L^{-1}, Yan et al., 2012, Changjiang River; range 0.04–0.48 mg N L^{-1}, Chen et al., 2014, Jiulong River), and agricultural groundwater (mean range = 0.00–3.22 mg N L^{-1}, Fenton et al., 2011, dairy farm Ireland; mean range = 0.00–3.30 mg N L^{-1}, McAleer et al., 2017, agricultural catchments Ireland). Based on excess N_2 concentrations, the mean loss of NO_3^- to N_2 was 68% along the 95 km section of the lower SJR, assuming the common respiratory denitrification pathway dominated N_2 production. The fraction of N_2 loss from DIN (NO_3^-, NH_4, NO_2) was somewhat lower at 46%; however this is higher than several previous studies from rivers surrounded by agricultural land such as Smith et al. (2006) (range 2–17%) and Chen et al. (2014) (mean range = 8–66%) have reported.

Excess N_2 within hyporheic porewaters showed a general pattern of increasing concentrations at downstream sites. Lower excess N_2 concentrations upstream of the Merced River confluence (118.5 km) possibly reflect differences in land use/land cover. Above the confluence, the predominant river-adjacent land uses are wetlands and grasslands. Below the confluence, agricultural activity increases on both the east and west sides of the river. Thus, we ascribe the general trend for increasing excess N_2 concentrations at downstream locations to a generally increasing pattern of nitrate leaching from agricultural intensification (Kratzer et al., 2011).

While mean excess N_2 showed a tendency to increase from the east to west side of the channel, the high variability within the stream cross section rendered these differences weakly significant ($p = 0.048$). Finer particle-size of sediments along the west-side likely hinders the diffusion of oxygen creating greater oxygen depletion and increased residence time, both of which can enhance denitrification (Harvey et al., 2013). This premise was supported by the percent loss of NO_3^- to excess N_2 as this percentage significantly ($p < 0.001$) increased from east to west (mean (%) = 48 ± 1, 68 ± 1, and 84 ± 1 for east, middle, and west bank positions, respectively). A previous study of NO_3^--rich seepage waters in west-side soils/sediments adjacent to the SJR showed rapid development of anoxic conditions and high rates of NO_3^- removal by denitrification in constructed wetlands (Brauer et al., 2015). Complicating the east- versus west-side comparison is the historical meandering of the river channel has resulted in a complex mixing of aquifer materials in the vicinity of the current river channel.

Excess N_2 was greater at the 1.82 m depth compared to 0.31 m at most sites, potentially indicating a vertical gradient where N_2 was diluted by hyporheic zone mixing of surface and ground waters (Jones and Mulholland, 2000). The negative relationship between O_2 and excess N_2, in addition to significantly lower O_2 concentrations at the deeper depth, supports the findings of several previous studies indicating denitrification in anaerobic conditions (Hill et al., 2000; Fenton et al., 2011; Chen et al., 2014). The negative relationship between temperature and N_2 is reflective of the deeper

Table 2
Surface water characteristics in the San Joaquin River, California in 2009.

Date	Site	EC (mS cm^{-1})	NO_3^--N (mg L^{-1})	NH_4^+-N (mg L^{-1})	pH
April 2009	201.7	1.05	0.27	0.01	8.00
	190.7	1.02	1.99	0.02	7.77
	173.5	1.00	1.58	0.01	8.02
	158.8	0.98	1.88	0.01	7.68
	135.0	0.75	2.70	0.03	8.00
	116.0	0.52	1.49	0.02	8.11
September 2009	201.7	0.83	0.15	0.03	7.73
	190.7	0.86	1.12	0.03	7.72
	173.5	0.88	2.76	0.08	7.72
	158.8	0.93	3.03	0.05	7.75
	135.0	0.67	2.22	0.02	7.75
	116.0	0.39	1.28	0.02	7.54

Table 3
Sediment characteristics in the six sites used from the denitrification potential experiment within the San Joaquin River in April and September 2009. Values represent the range, mean and standard error of two replicates.

April 2009	Sites	201.7		190.7		173.5		158.8		135		116	
TOC (%)	W	0.12–0.62	0.37 (0.35)	0.11–0.11	0.11 (0.00)	1.07–1.14	1.10 (0.01)	0.11–0.13	0.10 (0.00)	0.11–0.11	0.11 (0.00)	0.15–0.18	0.16 (0.02)
	M	0.09–0.10	0.09 (0.00)	0.10–0.11	0.11 (0.00)	0.10–0.12	0.11 (0.01)	0.91–0.91	0.91 (0.00)	0.12–0.14	0.13 (0.00)	0.13–0.15	0.15 (0.01)
	E	0.11–0.20	0.15 (0.05)	0.10–0.11	0.11 (0.00)	0.10–0.14	0.12 (0.02)	0.81–0.90	0.86 (0.06)	0.13–0.14	0.14 (0.00)	0.13–0.16	0.14 (0.01)
TN (%)	W	0.005 −0.066	0.036 (0.04)	<0.00 −0.004	0.002 (0.00)	0.115 −0.121	0.118 (0.00)	0.003 −0.004	0.004 (0.0)	<0.00 −0.006	0.003 (0.0)	0.008 −0.008	0.008 (0.00)
	M	<0.00 −0.006	0.003 (0.00)	<0.00 −0.003	0.002 (0.00)	0.004 −0.005	0.005 (0.00)	0.110 −0.109	0.109 (0.0)	0.005 −0.006	0.006 (0.0)	<0.00 −0.009	0.005 (0.00)
	E	0.009 −0.014	0.012 (0.00)	<0.00 −0.005	0.003 (0.00)	0.004 −0.009	0.007 (0.00)	0.077 −0.090	0.084 (0.0)	<0.00 −0.007	0.005 (0.0)	NA	NA
OxC (mg kg^{-1})	W	38.0–446	242 (289)	32.3–32.8	33.0 (0.36)	714–776	745 (44.0)	31.6–35.2	33.4 (2.54)	31.3–35.4	33.3 (2.91)	56.6–71.0	63.8 (10.1)
	M	40.5–37.1	38.8 (2.46)	33.6–15.2	39.4 (8.26)	30.2–46.7	38.4 (11.7)	632–669	651 (26.3)	32.8–36.1	34.4 (2.42)	34.2–54.0	44.1 (14.0)
	E	71.2–115	93.4 (31.2)	33.3–36.0	34.7 (1.88)	38.5–62.0	50.3 (16.6)	609–647	628 (26.4)	35.2–41.2	38.2 (4.21)	35.2–38.8	37.0 (2.54)
PSD (μm)	W	386–756	571 (262)	480–533	507 (37.4)	58.3–82.6	70.4 (17.2)	536–574	555 (26.9)	444–560	502 (82.1)	429–655	542 (160)
	M	526–595	560 (49.2)	490–515	502 (18.2)	657–661	659 (2.55)	60.3–67.3	63.8 (4.89)	560–666	613 (75.2)	525–656	591 (92.6)
	E	419–421	420 (1.56)	417–513	465 (68.2)	604–635	619 (21.8)	101–107	104 (3.53)	510–543	526 (23.3)	439–441	440 (1.20)
September 2009													
TOC (%)	W	0.30–0.42	0.36 (0.09)	0.05–0.14	0.10 (0.06)	0.84–1.25	1.04 (0.29)	0.10–0.14	0.12 (0.02)	0.09–0.09	0.09 (0.00)	0.08–0.08	0.08 (0.00)
	M	0.07–0.10	0.08 (0.02)	0.06–0.08	0.07 (0.02)	0.04–0.13	0.08 (0.06)	0.22–1.1	0.68 (0.71)	0.06–0.14	0.10 (0.06)	0.43–0.64	0.37 (0.39)
	E	0.15–0.32	0.23 (0.12)	0.05–0.34	0.20 (0.20)	0.09–0.15	0.12 (0.05)	0.79–1.0	0.88 (0.13)	0.05–0.05	0.05 (0.00)	0.06–0.43	0.25 (0.26)
TN (%)	W	0.041 −0.056	0.048 (0.01)	0.006 −0.020	0.013 (0.00)	0.088 −0.135	0.110 (0.03)	0.013 −0.023	0.018 (0.00)	0.005 −0.017	0.01 (0.00)	0.015 −0.016	0.016 (0.00)
	M	0.003 −0.014	0.009 (0.01)	0.004 −0.008	0.006 (0.00)	<0.00 −0.015	0.008 (0.01)	0.105 −0.131	0.078 (0.07)	<0.00 −0.021	0.01 (0.01)	0.015 −0.045	0.030 (0.02)
	E	0.018 −0.038	0.028 (0.01)	0.003 −0.038	0.0205 (0.02)	0.024 −0.008	0.021 (0.01)	0.085 −0.105	0.095 (0.01)	0.005–0.01	0.01 (0.00)	0.012 −0.033	0.022 (0.01)
OxC (mg kg^{-1})	W	298–590	444 (207)	60.9–61.2	61.1 (0.22)	683–909	796 (159)	88.8–137	113 (34.2)	85.6–104	95.1 (13.1)	68.1–71.4	70.0 (2.30)
	M	67.5–107	87.3 (27.9)	55.9–60.7	58.3 (3.43)	50.3–87.4	68.9 (26.3)	97.7–843	471 (528)	60.1–164	113 (74.1)	58.8–328	193 (190)
	E	168–342	255 (123)	72.3–207	139 (94.8)	84.3–140	112 (39.6)	684–806	745 (85.9)	61.8–65.7	63.8 (2.70)	58.4–146	102 (62.5)
PSD (μm)	W	171–612	392 (312)	515–625	570 (77.4)	67.3–158	113 (64.4)	501–627	564 (88.6)	476–586	531 (77.5)	599–660	630 (42.7)
	M	535–616	576 (57.6)	560–604	582 (31.3)	684–728	706 (30.3)	87.3–522	305 (308)	466–605	536 (98.0)	237–720	478 (342)
	E	284–319	302 (24.6)	345–495	420 (106)	519–614	567 (67.2)	61.0–90.6	75.81 (20.9)	426–471	448 (32.2)	647–674	660 (19.3)

TOC = Total organic carbon, TN = Total nitrogen, OxC = Oxidizable organic carbon and PSD = Particle size distribution.

depth being up to 4 °C cooler than the shallow depth, which also suggests that the deeper waters were sourced from deeper, regional groundwater (Zamora et al., 2012). This pattern further suggests that the shallow porewater is a combination of warmer surface waters mixing with cooler groundwater in the hyporheic zone. Thus, the vertical spatial differences in excess N_2 likely reflect water source (e.g., deep groundwater vs mixing of surface and ground waters in hyporheic zone) rather than inherent differences in *in situ* denitrification rates between the two depths. Models of surface water-groundwater interactions in the study area estimated that only about 10% of the surface waters during the summer low-flow season originates from groundwater inputs making groundwater a minor hydrologic source of surface waters overall (Zamora et al., 2012). Hence these findings support the suggestion above that the two depths represent different water sources.

Mixing of surface and ground waters at the 0.31-m depth is further supported by the higher SC values (mS cm^{-1}) at 1.82 m (mean = 2.96 ± 0.25) versus 0.31 m (mean = 2.43 ± 0.18), which suggest dilution of SC in the 0.31 m samples by surface waters that had a median SC of 0.98 mS cm^{-1} (Table S2). This would also suggest potential dilution and/or degassing of dissolved N_2 at the 0.31 m depth. Additionally, the negative correlation between excess

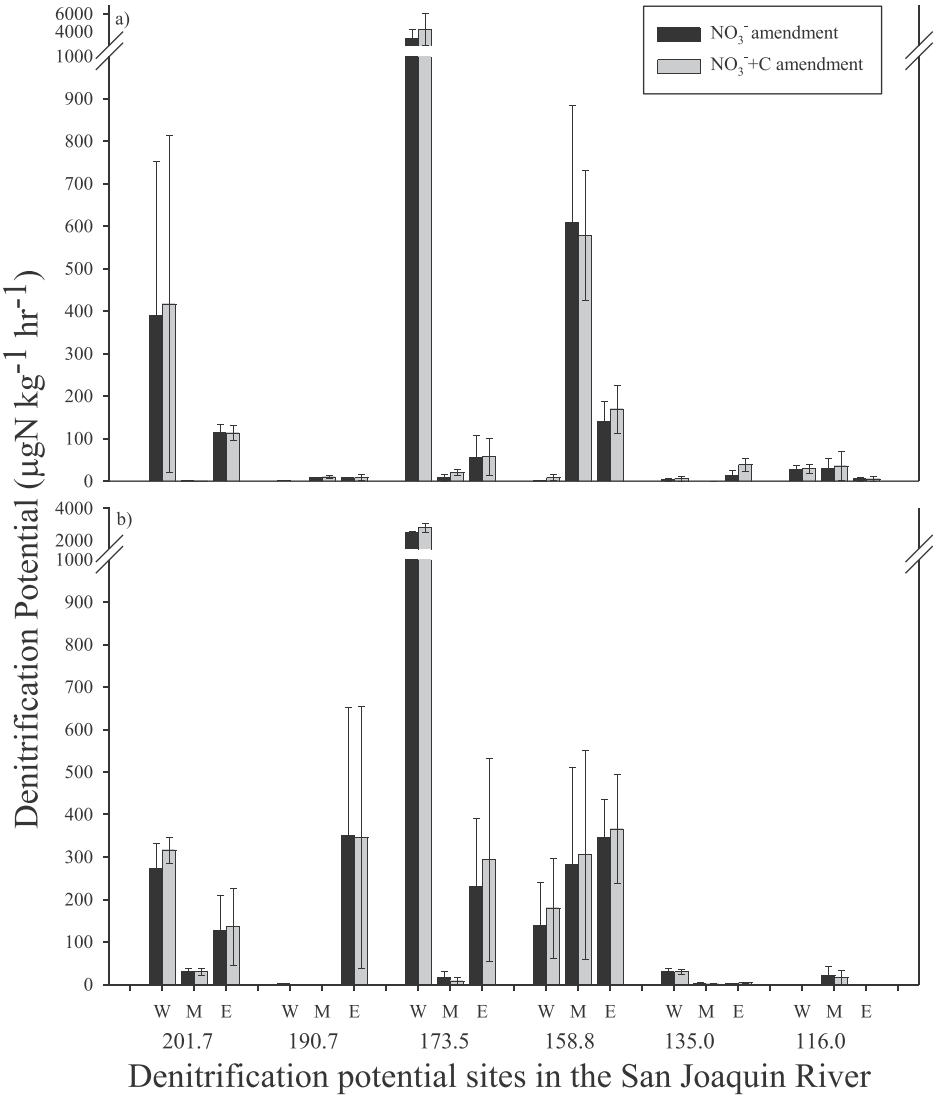

Fig. 5. Denitrification potential for a) April 2009 and b) September 2009. n = 4.

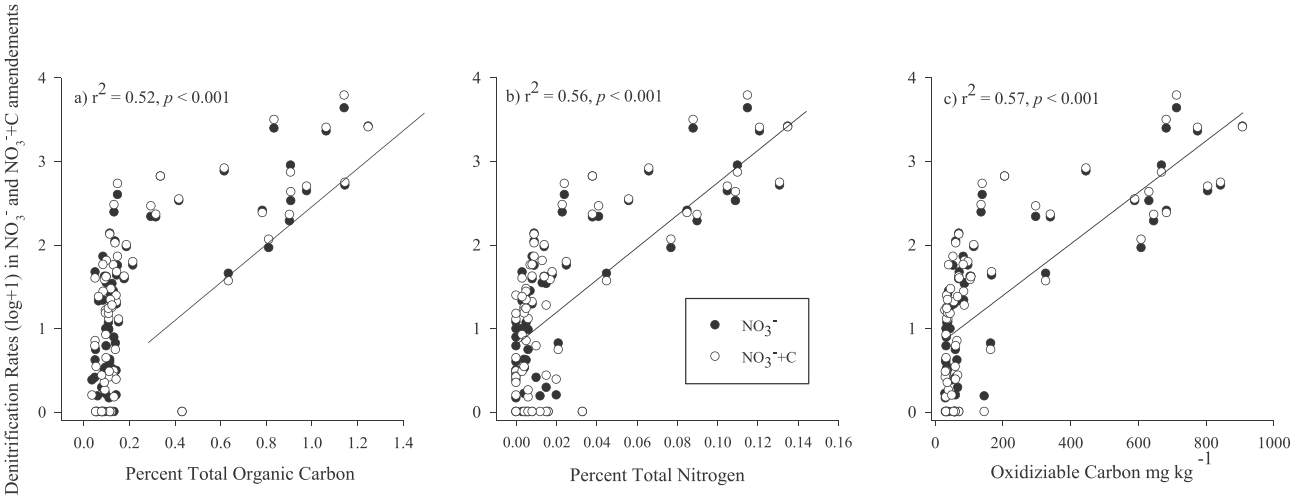

Fig. 6. Relationship between denitrification rates (log+1) in NO_3^- (closed circles) and NO_3^- + C amendments (open circles) with sediment (a) extracted percent total organic carbon, (b) percent total nitrogen and (c) oxidizable carbon.

N_2 in shallow but not deeper porewaters and NO_3^- in surface waters ($r = 0.41$, $p < 0.001$) supports the mixing of surface water/shallow porewater, while deeper hyporheic porewaters most likely originate from groundwater.

High spatial and temporal variability (hot spots—hot moments) commonly associated with denitrification processes was reflected at all spatial scales in this study (Bernard-Jannin et al., 2017). Rivers often switch between a nitrate sink and source due to upwelling of groundwater or downwelling of surface water within the hyporheic zone (Li et al., 2017). In this study, variability in excess N_2 was primarily associated with variations in NO_3^- and dissolved oxygen as depicted by the negative relationship between NO_3^- and excess N_2 when NO_3^- concentrations were >0.1 mg N L^{-1} (Fig. 4). This negative relationship was also found in the permanent groundwater wells screened between 3→7 m and in a previous study (Hinshaw and Dahlgren, 2016). This negative relationship is consistent with a dominant role for denitrification in consuming NO_3^- and producing excess N_2 gas.

Site 154.5 km was of particular interest given its high NO_3^- concentrations (10.2 ± 1.1 mg N L^{-1}) and low excess N_2 (<1 mg N L). This site is located just downstream of a wastewater treatment plant (tertiary treatment) located on the east bank. During the growing season (March—June), the majority of its treated effluent is disposed of as irrigation water for pastures that occur within 1 km of the river. Thus, large volumes of NO_3^--rich waters are added to the land surface, which presumably introduces localized NO_3^--rich groundwater having a relatively short residence time before emerging as surface waters in the SJR. Deep monitoring wells (13.2—16.8 m) within and surrounding the irrigated pasture were measured in the same manner as the riparian groundwater wells. The mean NO_3^- concentration was 6.1 mg N L^{-1} (range <0.01—23.8) and mean excess N_2 concentrations was 4.6 mg N L^{-1} (range = 1.35—8.92 mg N L^{-1}) (Table S4). Therefore, these deeper groundwaters do not appear to be the primary source of the hyporheic porewaters given their higher levels of excess N_2 and generally lower NO_3^- concentrations. Rather, we posit that a shallow groundwater flow path having insufficient residence time to allow for appreciable denitrification is the primary source of the hyporheic porewaters at site 154.5 km. Estimated groundwater flow rates of 0.03—0.12 $m^3 s^{-1}$ for the lower SJR could support a wide range of groundwater residence times (Zamora et al., 2012). Therefore, for this specific section of the SJR, higher flow rate/lower residence time flowpaths may prevent the onset of anoxic conditions, hindering denitrification and NO_3^- consumption.

Assuming sufficiently anaerobic conditions to support denitrification, or other mechanisms of N removal occurring under anaerobic conditions such as anammox or DNRA, groundwater sources will accumulate excess N_2 concentrations along the groundwater flowpath until either NO_3^- or DOC is depleted, which was supported by the mean concentration of excess N_2 in groundwater wells (7.18 ± 0.48) being nearly five times greater compared to the overall mean of excess N_2 concentrations within hyporheic porewaters (1.48 ± 0.14). Trauth et al. (2014) found that groundwater flow had a greater influence over denitrification rates than stream discharge and emphasized the importance of accounting for groundwater inputs into the hyporheic zone.

4.2. Denitrification potential rates

Denitrification potential rates were measured in the year following the longitudinal study to verify if denitrification was a prevalent process within hyporheic porewaters. Out of the 144 DNP incubations, 86% demonstrated denitrifying activity. Despite oxygenated mixing of surface water within the hyporheic zone, nitrification was considered negligible due to low or undetectable NH_4^+ within SJR surface waters (Hinshaw and Dahlgren, 2013). DNP rates displayed high spatial variability within sites, among sites, and between seasons (April vs September) as is often found in such studies. DNP rates were greater than those compared to a study in agriculturally impacted lakes (Liu et al., 2015) and those found in natural and forested wetlands (Gardner and White, 2010; Harrison et al., 2011; Genthner et al., 2013). The similarity between DNP rates in the NO_3^- + C amendments and NO_3^- originally suggests no appreciable carbon limitation for denitrifiers, in spite of the rather low total carbon concentrations (0.08—0.63%). This is consistent with several similar studies that found that NO_3^- and not organic carbon, limited sediment denitrification (Esteves et al., 2001; Wall et al., 2005). However, in this study stepwise regression suggested a positive contribution from OxC, owing to this fraction being most available for bacterial metabolism. The role of OxC is also supported by the data from site 173.5 km, which had the highest OxC concentrations (west) and the corresponding highest DNP rates. When NO_3^- concentrations are high, concentrations of OxC become more crucial for attenuating NO_3^- by stimulating denitrification activity and driving complete nitrate reduction to N_2 (Firestone et al., 1980). Similar results have been found in low carbon and elevated NO_3^- stream and river sediments (Bernhardt and Likens, 2002; Inwood et al., 2007; Findlay et al., 2011). Further, Xu et al. (2015) concluded that high organic matter is necessary to sustain low NO_3^- concentrations via denitrification in agricultural groundwater.

The relationship of higher DNP rates with lower PSD has been found in several previous studies (Pinay et al., 2000; Opdyke and David, 2007; Welsh et al., 2017). Similar to this study, D'Haene et al. (2003) found denitrification rates were highest in clay soil and lowest in sandy soils. Fine textured sediments, such as clay and silt, often harbor higher concentrations of carbon, lower oxygen concentrations and more suitable attachment sites for bacteria attenuating their downstream advection. Iribar et al. (2008) identified denitrifying bacteria communities attached to aquifer sediment that exhibited higher denitrification enzyme activity. The significantly higher DNP rates in NO_3^- and NO_3^- + C treatments from the east to west bank is consistent with the finer textured sediments resulting from the contrasting sediment sources (Table 2).

5. Conclusions

The predominantly elevated excess N_2 concentrations (and overall low NO_3^- concentrations (mean = 0.91 mg N L^{-1})in deeper porewaters suggest that the SJR riparian and hyporheic zones act as an effective anoxic barrier to NO_3^- transport from regional groundwaters to surface water. Sites with low or negligible N_2 tended to have high concentrations of NO_3^- and DO along with low DOC indicating inhibition of denitrification. DNP rates confirmed the prevalence of high denitrification capacity within hyporheic sediments of the SJR. Oxidizable C fraction was the key factor limiting DNP rates highlighting the importance of microbially labile C in fueling denitrification. This study suggests that riparian and hyporheic zone management and restoration activities that focus on increasing inputs of carbon and water transport residence times provide an opportunity for enhancing denitrification in hydrologic systems subject to high NO_3^- loading.

Declaration of competing interest

The authors declare that they have no known competing financial interests or personal relationships that could have appeared to influence the work reported in this paper.

Acknowledgments

This research was supported by US Geological Survey (USGS), Proposition 50 grant from the CALFED Drinking Water-Quality Program and from a contract with the US Bureau of Reclamation (R09AC20040). We thank Charles Kratzer, Peter Dileanis, Carol Kendall and Xien Wang for their field and laboratory assistance. Full data sets are available from Sarra Hinshaw.

Appendix A. Supplementary data

Supplementary data to this article can be found online at https://doi.org/10.1016/j.watres.2019.115161.

References

Bernhardt, E.S., Likens, G.E., 2002. Dissolved organic carbon enrichment alters nitrogen dynamics in a forest stream. Ecology 83 (6), 1689–1700. https://doi.org/10.1890/0012-9658(2002)083[1689:DOCEAN]2.0.CO;2.

Jones, J.B., Mulholland, P.J. (Eds.), 2000. Streams and Ground Waters. Academic Press.

Allen, D.E., Dalal, R.C., Rennenberg, H., Meyer, R.L., Reeves, S., Schmidt, S., 2007. Spatial and temporal variation of nitrous oxide and methane flux between subtropical mangrove sediments and the atmosphere. Soil Biol. Biochem. 39 (2), 622–631. https://doi.org/10.1016/j.soilbio.2006.09.013.

Bernard-Jannin, L., Sun, X., Teissier, S., Sauvage, S., Sánchez-Pérez, J.M., 2017. Spatio-temporal analysis of factors controlling nitrate dynamics and potential denitrification hot spots and hot moments in groundwater of an alluvial floodplain. Ecol. Eng. 103 (B), 372–384. https://doi.org/10.1016/j.ecoleng.2015.12.031.

Blicher-Mathiesen, G., McCarty, G.W., Nielsen, L.P., 1998. Denitrification and degassing in groundwater estimated from dissolved dinitrogen and argon. J. Hydrol. 208 (1–2), 16–24. https://doi.org/10.1016/S0022-1694(98)00142-5.

Brauer, N., Maynard, J.J., Dahlgren, R.A., O'Geen, A.T., 2015. Fate of nitrate in seepage from a restored wetland receiving agricultural tailwater. Ecol. Eng. 81, 207–217. https://doi.org/10.1016/j.ecoleng.2015.04.003.

Burgin, A.J., Hamilton, S.K., 2007. Have we overemphasized the role of denitrification in aquatic ecosystems? A review of nitrate removal pathways. Front. Ecol. Environ. 5 (2), 89–96. https://doi.org/10.1890/1540-9295(2007)5[89:HWOTRO]2.0.CO;2.

Burow, K.R., Stork, S.V., Dubrovsky, N.M., 1998. Nitrate and pesticides in ground water in the eastern san Joaquin valley, California : occurrence and trends. In: water-resources investigations report. U.S. Geological Survey, 98–4040A.

Chen, N., Wu, J., Chen, Z., Lu, T., Wang, L., 2014. Spatial-temporal variation of dissolved N_2 and denitrification in an agricultural river network, southeast China. Agric. Ecosyst. Environ. 189, 1–10. https://doi.org/10.1016/j.agee.2014.03.004.

D'Haene, K., Moreels, E., De Neve, S., Daguilar, B.C., Boeckx, P., Hofman, G., Van Cleemput, O., 2003. Soil properties influencing the denitrification potential of Flemish agricultural soils. Biol. Fertil. Soils 38 (6), 358–366. https://doi.org/10.1007/s00374-003-0662-x.

Doane, T.A., Howarth, R.W., 2003. Spectrophotometric determination of nitrate with a single reagent. Anal. Lett. 36 (12), 2713–2722. https://doi.org/10.1081/AL-120024647.

Eaton, A.D., Clesceri, L.S., Greenberg, A.E., Franson, M.A.H., 1998. Standard Methods for the Examination of Water and Wastewater, twentieth ed. American Public Health Association, Washington DC.

Esteves, F.A., Enrich-Prast, A., Biesboer, D.D., 2001. Potential denitrification in submerged natural and impacted sediments of Lake Batata, an Amazonian lake. Hydrobiologia 444 (1), 111–117. https://doi.org/10.1023/a:1017550729084.

Fenton, O., Healy, M.G., Henry, T., Khalil, M.I., Grant, J., Baily, A., Richards, K.G., 2011. Exploring the relationship between groundwater geochemical factors and denitrification potentials on a dairy farm in southeast Ireland. Ecol. Eng. 37 (9), 1304–1313. https://doi.org/10.1016/j.ecoleng.2011.03.025.

Findlay, S.E.G., Mulholland, P.J., Hamilton, S.K., Tank, J.L., Bernot, M.J., Burgin, A.J., et al., 2011. Cross-stream comparison of substrate-specific denitrification potential. Biogeochemistry 104 (1), 381–392. https://doi.org/10.1007/s10533-010-9512-8.

Firestone, M.K., Firestone, R.B., Tiedje, J.M., 1980. Nitrous oxide for soil denitrification: factors controlling its biological production. Science 208, 749–751. https://doi.org/10.1126/science.208.4445.749.

Forster, J.C., 1995. Methods in Applied Soil Microbiology and Biochemistry. Academic Press, UK.

Galloway, D.L., Riley, F.S., 1999. San Joaquin valley, California-largest human alteration of the earth's surface: in land subsidence in the United States. In: Galloway, D.L., Jones, D.R., Ingebritsen, S.E. (Eds.), U.S. Geological Survey, pp. 23–34. Vol. Circular 1182.

Galloway, J.N., Dentener, F.J., Capone, D.G., Boyer, E.W., Howarth, R.W., Seitzinger, S.P., et al., 2004. Nitrogen cycles: past, present, and future. Biogeochemistry 70 (2), 153–226. https://doi.org/10.1007/s10533-004-0370-0.

Gardner, L.M., White, J.R., 2010. Denitrification enzyme activity as an indicator of nitrate movement through a diversion wetland. Soil Sci. Soc. Am. J. 74 (3), 1037–1047. https://doi.org/10.2136/sssaj2008.0354.

Genthner, F.J., Marchovich, D.T., Lehrter, J.C., 2013. Estimating rates of denitrification enzyme activity in wetland soils with direct simultaneous quantification of nitrogen and nitrous oxide by membrane inlet mass spectrometry. J. Microb. Biochem. Technol. 5 (4), 95–101. https://doi.org/10.4172/1948-5948.1000108.

Groffman, P.M., Altabet, M.A., Bohlke, J.K., Butterbach-Bahl, K., David, M.B., Firestone, M.K., et al., 2006. Methods for measuring denitrification: diverse approaches to a difficult problem. Ecol. Appl. 16 (6), 2091–2122. https://doi.org/10.1890/1051-0761(2006)016[2091:MFMDDA]2.0.CO;2.

Harrison, J.A., Matson, P.A., Fendorf, S.E., 2005. Effects of diel oxygen cycle on nitrogen transformations and greenhouse gas emissions in a eutrophied subtropical stream. Aquat. Sci. 67 (3), 308–315. https://doi.org/10.1007/s00027-005-0776-3.

Harrison, M.D., Groffman, P.M., Mayer, P.M., Kaushal, S.S., Newcomer, T.A., 2011. Denitrification in alluvial wetlands in an urban landscape. J. Environ. Qual. 40 (2), 634–646. https://doi.org/10.2134/jeq2010.0335.

Harter, T., Dzurella, K., Kourakos, G., Hollander, A., Bell, A., Santos, N., et al., 2017. Nitrogen Fertilizer Loading to Groundwater in the Central Valley. Final Report to the Fertilizer Research Education Program, Projects 11-0301 and 15-0454. California Department of Food and Agriculture and University of California Davis, 325p.

Harvey, J.W., Böhlke, J.K., Voytek, M.A., Scott, D., Tobias, C.R., 2013. Hyporheic zone denitrification: controls on effective reaction depth and contribution to whole-stream mass balance. Water Resour. Res. 49 (10), 6298–6316. https://doi.org/10.1002/wrcr.20492.

Heaton, T.E., Vogen, J.C., 1981. Excess air in groundwater. J. Hydrol. 50, 201–216. https://doi.org/10.1016/0022-1694(81)90070-6.

Hill, A.R., Devito, K.J., Campagnolo, S., Sammugadas, K., 2000. Subsurface denitrification in a forest riparian zone: interactions between hydrology and supplies of nitrate and organic carbon. Biogeochemistry 51 (2), 193–223.

Hinshaw, S.E., Dahlgren, R.A., 2013. Dissolved nitrous oxide concentrations and fluxes from the eutrophic San Joaquin River, California. Environ. Sci. Technol. 47 (3), 1313–1322. https://doi.org/10.1021/es301373h.

Hinshaw, S.E., Dahlgren, R.A., 2016. Nitrous oxide fluxes and dissolved N gases (N_2 and N_2O) within riparian zones along the agriculturally impacted San Joaquin River. Nutrient Cycl. Agroecosyst. 105 (2), 85–102.

Holocher, J., Peeters, F., Aeschbach-Hertig, W., Hofer, M., Kipfer, R., 2002. Gas exchange in quasi-saturated porous media: investigations on the formation of excess air using noble gases. Geochem. Cosmochim. Acta 66 (15A). https://doi.org/10.1016/S0016-7037(02)00992-4. A338-A338.

Inwood, S.E., Tank, J.L., Bernot, M.J., 2007. Factors controlling sediment denitrification in midwestern streams of varying land use. Microb. Ecol. 53 (2), 247–258. https://doi.org/10.1007/s00248-006-9104-2.

Iribar, A., Sánchez-Pérez, J.M., Lyautey, E., Garabétian, F., 2008. Differentiated free-living and sediment-attached bacterial community structure inside and outside denitrification hotspots in the river–groundwater interface. Hydrobiologia 598 (1), 109–121. https://doi.org/10.1007/s10750-007-9143-9.

Ishida, C.K., Arnon, S., Peterson, C.G., Kelly, J.J., Gray, K.A., 2008. Influence of algal community structure on denitrification rates in periphyton cultivated on artificial substrata. Microb. Ecol. 56 (1), 140–152. https://doi.org/10.1007/s00248-007-9332-0.

James, W.F., Richardson, W.B., Soballe, D.M., 2008. Contribution of sediment fluxes and transformations to the summer nitrogen budget of an Upper Mississippi River backwater system. Hydrobiologia 598 (1), 95–107. https://doi.org/10.1007/s10750-007-9142-x.

Kana, T.M., Darkangelo, C., Hunt, M.D., Oldham, J.B., Bennett, G.E., Cornwell, J.C., 1994. Membrane inlet mass spectrometer for rapid high precision determination of N_2 and Ar in environmental samples. Anal. Chem. 66 (23), 4166–4170. https://doi.org/10.1021/ac00095a009.

Kartal, B., Kuypers, M.M.M., Lavik, G., Schalk, J., Op den Camp, H.J.M., Jetten, M.S.M., Strous, M., 2007. Anammox bacteria disguised as denitrifiers: nitrate reduction to dinitrogen gas via nitrite and ammonium. Environ. Microbiol. 9 (3), 635–642. https://doi.org/10.1111/j.1462-2920.2006.01183.x.

Knowles, R., 1982. Denitrification. Microbiol. Rev. 46 (1), 43–70.

Kratzer, C., Dileanis, P.D., Zamora, C., Silva, S.R., Kendall, C., Bergamaschi, B.A., Dahlgren, R., 2004. Sources and Transport of Nutrients, Organic Carbon, and Chlorophyll-A in the San Joaquin River *Water Resources Investigations* (Vol. Report 03-4127).

Kratzer, C.R., Kent, R.H., Saleh, D.K., Knifong, D.L., Dileanis, P.D., Orlando, J.L., 2011. Trends in Nutrient Concentrations, Loads, and Yields in Streams in the Sacramento, San Joaquin, and Santa Ana Basins, California, 1975–2004: U.S. Geological Survey Scientific Investigations Report, vols. 2010–5228, p. 112.

Kulkarni, M.V., Groffman, P.M., Yavitt, J.B., 2008. Solving the global nitrogen problem: it's a gas! Front. Ecol. Environ. 6 (4), 199–206. https://doi.org/10.1890/060163.

Li, Y., Wang, S., Zhang, W., Yuan, J., Xu, C., 2017. Potential drivers of the level and distribution of nitrogen in the hyporheic zone of Lake Taihu, China. Water 9 (7), 544. https://doi.org/10.3390/w9070544.

Liu, W., Yao, L., Wang, Z., Xiong, Z., Liu, G., 2015. Human land uses enhance sediment denitrification and N_2O production in Yangtze lakes primarily by influencing lake water quality. Biogeosciences 12 (20), 6059–6070. https://doi.org/10.5194/bg-12-6059-2015.

Lunstrum, A., Aoki, L.R., 2016. Oxygen interference with membrane inlet mass spectrometry may overestimate denitrification rates calculated with the isotope pairing technique. Limnol Oceanogr. Methods 14 (7), 425–431. https://doi.org/

10.1002/lom3.10101.
Marchant, H.K., Holtappels, M., Lavik, G., Ahmerkamp, S., Winter, C., Kuypers, M.M.M., 2016. Coupled nitrification–denitrification leads to extensive N loss in subtidal permeable sediments. Limnol. Oceanogr. 61 (3), 1033–1048. https://doi.org/10.1002/lno.10271.
McAleer, E.B., Coxon, C.E., Richards, K.G., Jahangir, M.M.R., Grant, J., Mellander, P.E., 2017. Groundwater nitrate reduction versus dissolved gas production: a tale of two catchments. Sci. Total Environ. 586, 372–389. https://doi.org/10.1016/j.scitotenv.2016.11.083.
Merill, L., Tonjes, D.J., 2014. A review of the hyporheic zone, stream restoration, and means to enhance denitrification. Crit. Rev. Environ. Sci. Technol. 44 (21), 2337–2379. https://doi.org/10.1080/10643389.2013.829769.
Muholland, P.J., Helton, A.M., Poole, G.C., Hall, R.O., Hamilton, S.K., Peterson, B.J., et al., 2008. Stream denitrification across biomes and its response to anthropogenic nitrate loading. Nature 452, 202–205.
O'Connor, B.L., Hondzo, M., 2008. Enhancement and inhibition of denitrification by fluid-flow and dissolved oxygen flux to stream sediments. Environ. Sci. Technol. 42 (1), 119–125. https://doi.org/10.1021/es071173s.
Opdyke, M.R., David, M.B., 2007. Response of sediment denitrification rates to environmental variables in streams heavily impacted by agriculture. J. Freshw. Ecol. 22 (3), 371–382. https://doi.org/10.1080/02705060.2007.9664166.
Pinay, G., Black, V.J., Planty-Tabacchi, A.M., Gumiero, B., Décamps, H., 2000. Geomorphic control of denitrification in large river floodplain soils. Biogeochemistry 50 (2), 163–182. https://doi.org/10.1023/A:1006317004639.
Puckett, L.J., Zamora, C., Essaid, H., Wilson, J.T., Johnson, H.M., Brayton, M.J., et al., 2008. Transport and fate of nitrate at the ground-water/surface-water interface. J. Environ. Qual. 37 (3), 1034–1050. https://doi.org/10.2134/jeq2006.0550.
Roland, F.A.E., Darchambeau, F., Borges, A.V., Morana, C., De Brabandere, L., Thamdrup, B., Crowe, S.A., 2018. Denitrification, anaerobic ammonium oxidation, and dissimilatory nitrate reduction to ammonium in an East African Great Lake (Lake Kivu). Limnol. Oceanogr. 63 (2), 687–701. https://doi.org/10.1002/lno.10660.
Schullehner, J., Hansen, B., Thygesen, M., Pedersen, C.B., Sigsgaard, T., 2018. Nitrate in drinking water and colorectal cancer risk: a nationwide population-based cohort study. Int. J. Cancer 143 (1), 73–79. https://doi.org/10.1002/ijc.31306.
Seitzinger, S.P., 1988. Denitrification in freshwater and coastal marine ecosystems: ecological and geochemical significance. Limnol. Oceanogr. 33 (4part2), 702–724. https://doi.org/10.4319/lo.1988.33.4part2.0702.
Seitzinger, S., Harrison, J.A., Bohlke, J.K., Bouwman, A.F., Lowrance, R., Peterson, B., 2006. Denitrification across landscapes and waterscapes: a synthesis. Ecol. Appl. 16 (6), 2064–2090. https://doi.org/10.1890/1051-0761(2006)016[2064:dalawa]2.0.co;2.
Smith, L.K., Voytek, M.A., Bohlke, J.K., Harvey, J.W., 2006. Denitrification in nitrate rich streams: application of N_2:Ar and ^{15}N-tracer methods in intact cores. Ecol. Appl. 16 (6), 2191–2207. https://doi.org/10.1890/1051-0761(2006)016[2191:DINSAO]2.0.CO;2.
Smith, R.L., Böhlke, J.K., Song, B., Tobias, C.R., 2015. Role of anaerobic ammonium oxidation (Anammox) in nitrogen removal from a freshwater aquifer. Environ. Sci. Technol. 49 (20), 12169–12177. https://doi.org/10.1021/acs.est.5b02488.
SPSS, 2001. SPSS for Windows: Version 20 (Chicago).
Strous, M., Fuerst, J.A., Kramer, E.H., Logemann, S., Muyzer, S., van de Pas-Schoonen, K.T., et al., 1999. Missing lithotroph identified as new planctomycete. Nature 400 (6743), 446–449. https://doi.org/10.1038/22749.
Tiedje, J.M., 1982. Denitrification. In: Page, A.L., Miller, R.H., Keeney, D.R. (Eds.), Methods of Soil Analysis, Part 2. Chemical and Microbiological Properties. American Society of Agronomy, Madison, Wisconsin, pp. 1011–1026.
Tomich, T.P., Brodt, S., Dahlgren, R.A., Scow, K.M., 2016. The California Nitrogen Assessment - Challenges and Solutions for People, Agriculture, and the Environment. University of California Press, Oakland, CA.
Townsend, A.R., Howarth, R.W., Bazzaz, F.A., Booth, M.S., Cleveland, C.C., Collinge, S.K., et al., 2003. Human health effects of a changing global nitrogen cycle. Front. Ecol. Environ. 1 (5), 240–246. https://doi.org/10.1890/1540-9295(2003)001[0240:HHEOAC]2.0.CO;2.
Trauth, N., Schmidt, C., Vieweg, M., Maier, U., Fleckenstein, J.H., 2014. Hyporheic transport and biogeochemical reactions in pool-riffle systems under varying ambient groundwater flow conditions. J. Geophys. Res.: Biogeosciences 119 (5), 910–928. https://doi.org/10.1002/2013JG002586.
U.S. Geological Survey, 2011. USGS #11303500 on the San Joaquin River Near Vernalis, CA: Annual Water-Data Report, 1924–2011:National Water Information System.
Wall, L.G., Tank, J.L., Royer, T.V., Bernot, M.J., 2005. Spatial and temporal variability in sediment denitrification within an agriculturally influenced reservoir. Biogeochemistry 76 (1), 85–111. https://doi.org/10.1007/s10533-005-2199-6.
Weil, R.R., Islam, K.R., Stine, M.A., Gruver, J.B., Samson-Liebig, S.E., 2003. Estimating active carbon for soil quality assessment: a simplified method for laboratory and field use. Am. J. Altern. Agric. 18 (1), 3–17. https://doi.org/10.1079/AJAA200228.
Weiss, R.F., Price, B.A., 1980. Nitrous oxide solubility in water and seawater. Mar. Chem. 8 (4), 347–359. https://doi.org/10.1016/0304-4203(80)90024-9.
Welsh, M.K., McMillan, S.K., Vidon, P.G., 2017. Denitrification along the stream-riparian continuum in restored and unrestored agricultural streams. J. Environ. Qual. 46 (5), 1010–1019. https://doi.org/10.2134/jeq2017.01.0006.
Weymann, D., Well, R., Flessa, H., von der Heide, C., Deurer, M., Meyer, K., Walther, W., 2008. Assessment of excess N_2 and groundwater N_2O emission factors of nitrate-contaminated aquifers in northern Germany. Biogeosci. Discuss. 5 (2), 1263–1292. https://doi.org/10.5194/bgd-5-1263-2008.
Xu, Z., Wang, Y., Li, H., 2015. Stoichiometric determination of nitrate fate in agricultural Ecosystems during rainfall events. PLoS One 10 (4), e0122484. https://doi.org/10.1371/journal.pone.0122484.
Yan, W., Yang, L., Wang, F., Wang, J., Ma, P., 2012. Riverine N_2O concentrations, exports to estuary and emissions to atmosphere from the Changjiang River in response to increasing nitrogen loads. Glob. Biogeochem. Cycles 26 (4). https://doi.org/10.1029/2010GB003984.
Zamora, C., Dahlgren, R.A., Kratzer, C.R., Downing, B.D., Russell, A.D., Dileanis, P.D., et al., 2012. Groundwater Contributions of Flow, Nitrate, and Dissolved Organic Carbon to the Lower San Joaquin River, California, during 2006-2008. Geological Survey, Reston, Virginia U.S.
Zarnetske, J., Haggerty, R., Wondzell, S.M., Baker, M.A., 2011. Dynamics of nitrate production and removal as a function of residence time in the hyporheic zone. J. Geophys. Res.: Biogeosciences 116 (G1). https://doi.org/10.1029/2010JG001356.